

Modeling of Precipitation in Reverse Micellar Systems

Rajdip Bandyopadhyaya, R. Kumar,[†] and K. S. Gandhi*

Department of Chemical Engineering, Indian Institute of Science, Bangalore 560 012, India

D. Ramkrishna*

School of Chemical Engineering, Purdue University, West Lafayette, Indiana 47907

Received June 17, 1996. In Final Form: March 12, 1997[Ⓢ]

A model of the precipitation process in reverse micelles has been developed to calculate the size of fine particles obtained therein. While the method shares several features of particle nucleation and growth common to precipitation in large systems, complexities arise in describing the processes of nucleation, due to the extremely small size of a micelle and of particle growth caused by fusion among the micelles. Occupancy of micelles by solubilized molecules is governed by Poisson statistics, implying most of them are empty and cannot nucleate of its own. The model therefore specifies the minimum number of solubilized molecules required to form a nucleus which is used to calculate the homogeneous nucleation rate. Simultaneously, interaction between micelles is assumed to occur by Brownian collision and instantaneous fusion. Analysis of time scales of various events shows growth of particles to be very fast compared to other phenomena occurring. This implies that nonempty micelles either are supersaturated or contain a single precipitated particle and allows application of deterministic population balance equations to describe the evolution of the system with time. The model successfully predicts the experimental measurements of Kandori *et al.*³ on the size of precipitated CaCO₃ particles, obtained by carbonation of reverse micelles containing aqueous Ca(OH)₂ solution.

1. Introduction

The preparation of fine particles of nanometer dimensions is currently of considerable technological interest. One of the methods of preparation of these particles is to precipitate them in swollen reverse micelles, which act as microreactors. Large scale production of fine CaCO₃ particles has been achieved for motor oil application,¹ for example, by passing CO₂ through an oil medium in which reverse micelles containing aqueous Ca(OH)₂ solution as well as Ca(OH)₂ added in the form of micron-sized particles are dispersed. The swollen reverse micelles are usually generated beforehand by reaction between a sulfonic acid and the dispersed Ca(OH)₂ particles, producing both the surfactant and water. Roman *et al.*² have investigated the formation of CaCO₃ nanoparticles on carbonation of a suspension of micron-sized Ca(OH)₂ particles in oil. Prior to carbonation, the suspension was reacted with sulfonic acid, and methanol was added to the medium. Thus, calcium salt of the surfactant and reverse micelles were formed in situ. These reverse micelles continually solubilize Ca(OH)₂ from the suspended particles. The resulting aqueous pools containing Ca(OH)₂ solution then yields CaCO₃ particles on reaction with CO₂. Apart from the nucleation and growth of CaCO₃ particles, which are associated with bulk precipitation also, other phenomena coming into play here are the dissolution of Ca(OH)₂ from the particles to the reverse micelles and the intermicellar Brownian collision process. The latter results in exchange of material between the micelles. The process of nucleation in a micelle also becomes more complex because of their extremely small size of a few nanometers and the nonuniform distribution of Ca(OH)₂ molecules in them.

Following a similar but simplified procedure, Kandori *et al.*³ precipitated CaCO₃ particles from reverse micelles containing dissolved Ca(OH)₂. Here the solubilization step

is eliminated since Ca(OH)₂ particles were not added. Nucleation and growth of particles in swollen reverse micelles therefore form the central features in the particle formation process. Unlike in the investigation of Roman *et al.*,² here the water to surfactant (CaOT) molar ratio (*R*) as also the concentration of aqueous Ca(OH)₂ solution in the pools of reverse micelles were varied. One of the interesting conclusions of Kandori *et al.*³ is that nearly 10⁸ reverse micelles present initially contribute to form one CaCO₃ particle in the end.

The purpose of the present investigation is to develop an understanding of the controlling mechanisms in the formation of particles by modeling the precipitation process in appropriate quantitative detail. The resulting models would play a significant role in the control of precipitation processes with respect to particle size, composition, and so on. In view of the relative simplicity of the process followed by Kandori *et al.*,³ explanation of their results on particle size was taken up as the objective of the present work.

2. The Model

The system investigated by Kandori *et al.*³ has the following features. Initially, the medium consists of reverse micellar pools containing Ca(OH)₂ molecules. Rapid collision among these micelles ensures that an equilibrium distribution of the number of Ca(OH)₂ molecules in various micelles is established in the beginning. The distribution is usually assumed to be Poissonian.⁴ The number of micelles being more than the number of Ca(OH)₂ molecules, most of the micelles are devoid of the hydroxide. Subsequently when CO₂ is bubbled through the system, it is transferred to the organic cyclohexane phase from where it dissolves into the micelles, supersaturating their water pools with respect to CaCO₃, whenever enough molecules of Ca(OH)₂ are present.

* Author to whom correspondence should be addressed.

[†] Also at Jawaharlal Nehru Centre for Advanced Scientific Research, Bangalore, India.

[Ⓢ] Abstract published in *Advance ACS Abstracts*, May 1, 1997.

(1) Marsh, J. F. *Chem. Ind.* **1987**, 14, 470.

(2) Roman, J.; Hoornaert, P.; Faure, D.; Biver, C.; Jacquet, F.; Martin, J. *J. Colloid Interface Sci.* **1991**, 144, 324.

(3) Kandori, K.; Kon-No, K.; Kitahara, A. *J. Colloid Interface Sci.* **1988**, 122, 78.

(4) Infelta, P. P.; Gratzel, M. J. *J. Chem. Phys.* **1979**, 70, 179. Dorrance, R. C.; Hunter, T. F. *J. Chem. Soc., Faraday Trans.* **1974**, 70, 1572.

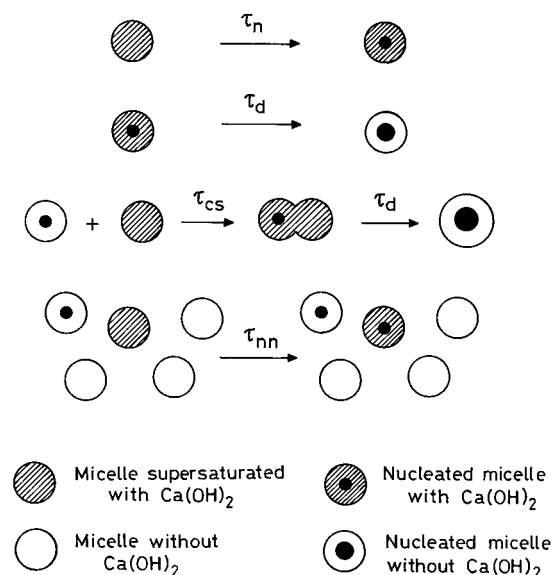


Figure 1. Schematic representation of various events during precipitation.

Nuclei of CaCO_3 form in supersaturated micelles, but at different times due to the randomness of the nucleation phenomenon. The nuclei so formed initially grow by consuming the supersaturation of the micelles in which they have been created. Simultaneously with this process, collision and fusion of micelles also occur due to Brownian motion. In this process if a supersaturated micelle collides and fuses with a micelle containing a CaCO_3 particle, the resulting supersaturation could create a new nucleus and also contribute to the growth of the pre-existing nucleus. The former process can then generate a distribution in the number of particles a single micelle can have. We wish to show that the extremely small size of a micelle precludes creation of such a distribution in the particle population inside a micelle, and it is this feature which permits considerable simplification of the theory of particle formation.

2.1. Time Scale Analysis. Although the overall process involves the formation of nuclei in micelles having supersaturation and their growth by using up supersaturation existing in themselves as well of other micelles through the processes of collision and fusion, the detailed process depends on the rates of various subprocesses involved. These various processes occurring in the system are shown schematically in Figure 1. The relative rates of these various processes can lead to different models of the overall process. The main time scales which decide the sequence of various events are as follows:

τ_n = time scale for nucleation. It is the time elapsed between formation of successive nuclei in the same micelle.

τ_d = time scale for depletion. It is the time required to remove supersaturation in a single nucleated micelle by growth of the nucleus.

τ_c = collision time scale. It is the time interval between two sequential collisions a particular micelle encounters.

τ_e = exchange time scale. It is the time allowed for two collided micelles to exchange their contents.

τ_{nn} = time elapsed between nucleation in the micellar phase as a whole.

When $\tau_n \approx \tau_c \approx \tau_d \approx \tau_e$, both collision and further nucleation can occur before the supersaturation existing in a micelle has been depleted and can lead to a distribution of particles in a single micelle. Investigation of such a situation would therefore entail simultaneous and interactive analysis of all the processes influencing the behavior

of a single micelle. Manjunath *et al.*⁵ investigated such a system but in the absence of fusion and exchange between micelles.

If on the other hand, $\tau_n > \tau_c > \tau_e > \tau_d$, then because of the smallness of τ_d before a nucleated micelle undergoes another collision, its supersaturation is completely exhausted by growth of the existing nucleus. No further nucleation can therefore occur during this period of growth. Subsequently, when this nucleated micelle collides with a supersaturated but non-nucleated one, the resulting supersaturation leads to growth of the pre-existing nucleus. This would lead to a situation where a micelle can have only one nucleation event and can further grow stepwise with each successive collision involving a supersaturated micelle. Thus the various processes of nucleation, particle growth, and further growth due to collision proceed in a noninteractive, sequential fashion. The analysis of this process is much easier.

Yet another situation may arise when, $\tau_n \geq \tau_c \gg \tau_d > \tau_{nn}$. In this case, the supersaturation in a single nucleated micelle will get exhausted before either the next nucleus gets formed in it or the collision changes its supersaturation. In such a case a large number of small particles can be expected.

Interestingly, when $\tau_e \gg \tau_c$, a number of micelles may be simultaneously participating in the process of material exchange by collision.

Thus, the relative values of different time scales can lead to different behavioral patterns of the nucleation cum growth phenomena in reverse micelles. We now proceed to calculate the above time scales for the experiments of Kandori *et al.*³

The collision time scale can be calculated using the concepts of Brownian motion. Consider a suspension of two types of particles with and without nuclei with number densities n_1 and n_2 . The Brownian collision frequency between these two types of particles in a solution of volume v is given by

$$(8k_B T/3\eta)n_1n_2v$$

In this work we will be concerned with the frequency of collision between a chosen member of one population with any other member of another or the same population. This can be calculated easily from the above. Consider a reverse micelle population with a number density of n_1 . A chosen micelle will collide with any other reverse micelle at a frequency of

$$(8k_B T/3\eta) \frac{1}{v} n_1 v = (8k_B T/3\eta)n_1$$

The time scale for such collisions due to Brownian motion is therefore given by

$$\tau = (3\eta/8k_B T) \frac{1}{n_1} \quad (1)$$

For the experiments of Kandori *et al.*,³ the number density of reverse micelles is of the order of 10^{18} cm^{-3} and the Brownian collision frequency is $10^{-11} \text{ cm}^3 \text{ s}^{-1}$ at the temperature of the experiment. The time between two collisions undergone by a particular micelle, denoted by τ_{cb} , is therefore 10^{-7} s . It is this high collision frequency which maintains the equilibrium Poisson distribution, referred to earlier. Let τ_{cs} be the time interval between successive collisions a nucleated micelle undergoes with supersaturated micelles. We will see shortly that, τ_{cs} is

(5) Manjunath, S.; Gandhi, K. S.; Kumar, R.; Ramkrishna, D. *Chem. Eng. Sci.* **1994**, *49*, 1451.

at least greater than τ_{cb} by one order. So for the purposes of calculating growth due to such collision, it is sufficient to characterize the non-nucleated micelle population at its Poisson distribution.

For calculating the nucleation time scale, it is assumed that the nucleation events occur in the micelles in such a way that the average rate of nucleation in an ensemble of micelles, having the same amount of $\text{Ca}(\text{OH})_2$ in each of them, corresponds to nucleation rate in a large system, having the same concentration. The time intervals between nucleation events in different micelles and in the same micelle, respectively, have been calculated as follows.

An aqueous solution of $\text{Ca}(\text{OH})_2$ and CO_2 , saturated with respect to both, produces a supersaturation of about 50 (see eq 33). The nucleation rate in a micelle of size 100 Å calculated at this level of supersaturation is of the order of 10^{-10} s^{-1} .

Thus for the experiments of Kandori *et al.*³ the time interval between nucleating events in different micelles works out to be $\tau_{nn} \approx 10^{-8} \text{ s}$, whereas its value for the same reverse micelle is a huge $\tau_n \approx 10^{10} \text{ s}$, thus indicating that nucleation events in a single micelle are very rare.

Time required for exhausting the supersaturation in a single reverse micelle by growth of the nucleus can also be evaluated. The maximum hydrodynamic diameter of micelles used by Kandori *et al.*³ was of the order of 100 Å. Suppose we assume that the water pool of the micelle is also of the same size. Thus if a particle and a calcium atom coexist in a micelle, they will collide with each other due to Brownian motion, resulting in growth, in about 10^{-7} s . Thus, supersaturation is expected to be dissipated by growth in about 10^{-7} s . The water pool is of course less than 100 Å in size, and hence the time required for growth and dissipation of supersaturation is smaller than this. In fact the time of growth of a particle τ_d works out to be less than 10^{-8} s .

On comparison we find that, as $\tau_d \ll \tau_n$, when a nucleus forms in a given micelle, the entire supersaturation is consumed quickly leading to the formation of a CaCO_3 particle, and the water pool would be left saturated with respect to CaCO_3 .⁶ From the above argument we conclude that multiple nucleation in a single micelle can be ruled out.

There could however be another way in which a second particle can be created in a given micelle. There will be collisions occurring between a supersaturated micelle and a micelle containing a particle, leading to the formation of a fused micelle. Such collisions will lead to creation of supersaturation in the fused micelle since the particle-containing micelle is previously saturated with respect to CaCO_3 . If these events occur very frequently, it is possible that supersaturation can build up in the fused micelle and another nucleus can form. Such is possible if the time required for the particle to grow, and hence dissipate the supersaturation, is larger than the time interval elapsing between successive collisions of the micelle-containing particle with supersaturated micelles. Now we will estimate these time scales. Using the Poisson distribution, with average number of $\text{Ca}(\text{OH})_2$ molecules per micelle as its mean, the fraction of micelles containing one or more of calcium atoms can be calculated to be about 0.1 (or less) of the entire micelle population. This corresponds to the conditions employed by Kandori *et al.*³ with R decreasing from 20 to less. As precipitation continues, this fraction further goes down due to de-

ing amounts of $\text{Ca}(\text{OH})_2$ available in the whole system. Therefore, supersaturated micelles that contain calcium atoms are present in the beginning at a maximum concentration of about 10^{17} per cm^3 of solution. Hence, a particle-containing micelle will collide and fuse with a micelle that is supersaturated, at a time interval of 10^{-6} s .⁷ Furthermore, this is an estimate of the shortest time interval between such collisions. As the number of micelles containing $\text{Ca}(\text{OH})_2$ molecules decreases due to continuous precipitation, this time interval also increases. We then have the minimum value of $\tau_{cs} \approx 10^{-6} \text{ s}$, which is more than the maximum growth time scale of $\tau_d \approx 10^{-8} \text{ s}$. Therefore for this worst case comparison also, it can be concluded that when a micelle containing a particle fuses with a supersaturated micelle, the resulting supersaturation is consumed very quickly leading to the growth of the existing particle, ruling out the formation of a second nucleus.

There still exists a possibility that a particle while growing meets a micelle with no calcium atoms and its supersaturation is redistributed before growth is complete. However, this collision time scale τ_{cb} , as we found previously, is 10^{-7} s and is therefore more than the growth time scale τ_d of 10^{-8} s . So for our purposes growth of a particle is always complete before any kind of further collision takes place.

The comparison of time scales then finally shows that $\tau_n \gg \tau_{cs} > \tau_{cb} > \tau_d$. This indicates that (i) a reverse micelle will give rise to a single nucleus at a time, which by the time it collides with another micelle, would completely exhaust its supersaturation and (ii) any collision and fusion of a particle-containing micelle with a supersaturated micelle also leads only to particle growth, consuming the supersaturation, and not to the creation of another nucleus. Thus, once a nucleus appears, it immediately gets converted into a particle before the existing supersaturation can increase or decrease due to collision with any other micelle, supersaturated or not. Subsequently growth of this particle also occurs as a result of collision with micelles having supersaturation but without particles.

We further assume that collision of two micelles having a particle in each does not result in a micelle having two particles. We note that in this case, calcium imbalance does not exist between them and there is no driving force for fusion.

On the basis of the above rationale, because of the formation of only a single nucleus in a micelle and its instantaneous growth both from within and also due to the collisions with other supersaturated micelles, it is possible to describe the whole process of nucleation and growth in a deterministic framework, and the stochastic elements arising out of multiple nucleation in a single micelle as in the work of Manjunath *et al.*⁵ are obviated. Furthermore, this eliminates from our analysis the need of any growth kinetics and consequent dynamics of particle size.

Summarizing, the overall process describing the Kandori *et al.*³ experiment can be assumed to proceed as follows. Before the passage of CO_2 , the swollen reverse micelles have the same size but a Poisson distribution in terms of the number of $\text{Ca}(\text{OH})_2$ molecules each micelle holds. When CO_2 is passed, it dissolves in the organic phase, transferring therefrom to the aqueous pools of the reverse micelles. The ionic reactions proceed there resulting in supersaturation that is also distributed. This

(6) It should be mentioned that the solubility of CaCO_3 is so small that for all practical purposes the saturated water pool of a reverse micelle can be considered to contain no calcium at all.

(7) In literature,¹⁷ based on some measurements, this time scale has been estimated to be of the order of 100 μs . The difference between this and our estimate arises since every collision may not lead to fusion. It may be noted that our conclusions are only justified by these estimates.

leads to the formation of nuclei as per nucleation theory in the bulk, having the same supersaturation as a particular micelle. Nucleation then divides the micelles into two categories—those having nuclei and the others which do not have. As precipitation continues, the numbers of both change with time. Time scale analysis shows that as soon as a nucleus is formed in a micelle, it exhausts all the supersaturation present therein instantaneously. Similar is the case when a supersaturated micelle collides with it, leading to further particle growth. The extent of growth possible by a particular collision is thus always complete prior to further collision with any other kind of micelle—supersaturated or not. We, however, assume that collision of two nucleated micelles has no effect. Thus the purpose of the model is to evaluate the number of nucleated micelles as well as the size of the particles as a function of time.

2.2. Number Densities. From the discussion above, there clearly is a need at the outset to distinguish between nucleated and non-nucleated micelles. The population of non-nucleated micelles can be characterized as follows. The experimental conditions specify the molar ratio of water to surfactant used, as well as the number of micelles per unit volume of the system. Hence, the size of the water core of the reverse micelles was calculated, assuming monodisperse population. Furthermore, the initial amount of calcium hydroxide in the system was also specified. Therefore the average number of calcium atoms per micelle, arising from calcium hydroxide present, is estimated.⁸ Typically, this number is fractional and small. According to Poisson distribution then, the number of non-nucleated micelles containing a large number of calcium atoms is extremely small. It is therefore convenient to characterize the non-nucleated micelle population by the number of calcium atoms contained in them. If the resulting number of calcium ions generated by ionic reactions in different non-nucleated micelles is calculated, the supersaturation generated in each of these due to absorption and desorption of CO₂ can also be obtained.

Since growth is regarded as instantaneous, a nucleated micelle must immediately have a particle with all the realizable mass from the available supersaturation within that micelle. Moreover since no further nucleation is permitted to occur, every nucleated micelle may be regarded as mononucleated. For simplicity we refer to them as nucleated micelles. The mass of an existing particle in a nucleated micelle increases upon collision and fusion with a non-nucleated micelle by an amount equivalent to the supersaturation prevailing in the latter. The mass of the particle is directly related to the number of calcium atoms in it. Hence, the number of calcium atoms in the particle can be used as the variable that characterizes the nucleated micelles.

Here we have assumed that the reverse micelles are uniformly distributed in size. This assumption can be avoided, but inclusion of this detail would increase the computational complexity of this preliminary model needlessly.

We require two basic functions $n_0(i, t)$ and $n_1(i, t)$ to characterize the populations of non-nucleated micelles and the nucleated micelles, respectively. $n_0(i, t)$ is the number of non-nucleated micelles per unit volume of the system

which contain i number of calcium atoms, whereas $n_1(i, t)$ is the number of nucleated micelles per unit volume of the system containing a particle composed of i number of calcium atoms. The total number density functions are then given by

$$N_1(t) = \sum_{i=1}^{\infty} n_1(i, t) \quad (2)$$

$$N_0(t) = \sum_{i=0}^{\infty} n_0(i, t) \quad (3)$$

Assuming Poisson distribution, it follows that

$$n_0(i, t) = N_0(t) P_i(t), \quad i = 0, 1, 2, 3, \dots \quad (4)$$

where $P_i(t)$ is the probability that i number of calcium atoms are present in a non-nucleated micelle and is given by

$$P_i(t) = \frac{\overline{Ca(t)}^i \exp[-\overline{Ca(t)}]}{i!}, \quad i = 0, 1, 2, 3, \dots \quad (5)$$

In the above equation, $\overline{Ca(t)}$ is the average number of calcium atoms in the non-nucleated micelles at any given time. The population of non-nucleated micelles for i greater than 6 is extremely small since $\overline{Ca(t)}$ is fractional. Hence, the sum in the eqs 2 and 3 can be truncated after a small number of terms.

2.3. Population Balance Equations. The foregoing number density functions will satisfy suitable population balance equations which are readily identified when more assumptions specific to the model are formulated. Let the nucleated and non-nucleated micelles collide with a frequency q . We assume this to be given by the Brownian collision frequency, as given by Smoluchowski.⁹ For the sake of simplicity, we consider the collision to be that between equal sized micelles, which is a reasonable assumption as the micelles are not broadly distributed in size. Furthermore, all such collisions are assumed to lead to mixing of drop contents. We therefore have

$$q = 8k_B T/3\eta \quad (6)$$

As mentioned earlier, we assume that the rate of transition probability of non-nucleated micelles to nucleated micelles is given by the rate of nucleation observed in a large scale system at the corresponding level of supersaturation. Let the rate of transition probability of a non-nucleated micelle containing i calcium atoms be represented by $k_i(t)$.

We have earlier shown the non-nucleated micelles to be colliding with each other very rapidly, which allows us to assume that the equilibrium Poisson distribution in terms of the available calcium atoms is maintained. Therefore, it is not necessary to solve the population balance equation for $n_0(i, t)$ in order to obtain the explicit distribution of non-nucleated micelles. Instead it is sufficient to work with only moments of that equation, which describe the change in number of micelles and calcium available for precipitation. The zeroth moment, for example, gives the total number of non-nucleated micelles, the rate of change of which is given by

(8) The calcium of the surfactant is present mostly at the surface of the micelle and is tightly bound to the polar sulfonate head of the surfactant. Hence, it is assumed that this does not participate in the precipitation reactions, and for these purposes, only the calcium arising from the calcium hydroxide need be considered. This is distributed in various calcium-containing species due to fast ionic reactions. For example, the total count of such calcium atoms initially is given by the sum of Ca²⁺, Ca(OH)⁺, and Ca(OH)₂(aq).

(9) Smoluchowski, M. V. *Phys. Z.* **1916**, *17*, 557.

$$\frac{dN_0(t)}{dt} = -\sum_{i=1}^{\infty} k_i(t) n_0(i, t) - qN_1(t) \sum_{i=1}^{\infty} n_0(i, t) \quad (7)$$

The first term on the right hand side of the above equation represents the rate of transition of non-nucleated micelles into a nucleated state, and consequent decrease in the number of the former kind. Obviously, only micelles having at least one molecule of $\text{Ca}(\text{OH})_2$ can possibly nucleate. This is reflected in omission of $i = 0$ from the sum. This will be further elucidated when the expression for $k_i(t)$ is discussed later. The second term represents loss of non-nucleated micelles due to fusion with the nucleated kind. In this term we exclude collisions with "blank" non-nucleated micelles ($i = 0$), those which do not contain any soluble calcium and hence do not allow any growth in the particle. The following population balance equation can now be written for nucleated micelles.

$$\frac{dn_1(i, t)}{dt} = k_i(t) n_0(i, t) - qn_1(i, t) \sum_{j=1}^{\infty} n_0(j, t) + q \sum_{\substack{j=1 \\ i \geq 2}}^{i-1} n_1(j, t) n_0(i-j, t) \quad (8)$$

$$i = 1, 2, 3, \dots$$

The first term on the right hand side gives generation of nucleated micelles of size i . The second term represents loss due to growth of the particle size i when fusion with any calcium-containing non-nucleated micelle occurs, whereas the last term accounts for gain due to formation of a micelle containing a particle of size i during fusion between a nucleated and a non-nucleated micelle of appropriate calcium contents. While writing the above equations, we have neglected the number of calcium atoms corresponding to saturation of CaCO_3 as mentioned previously.

The number of micelles containing a particle and the average mass of the particle in terms of the number of Ca atoms i need to be calculated from the model for the purposes of comparison with the experimental observations. Hence we work with the relevant moment equations, derived from eq 8. The zeroth moment of this is $N_1(t)$, giving the number of nucleated micelles. The governing equation is as follows.

$$\frac{dN_1(t)}{dt} = \sum_{i=1}^{\infty} k_i(t) n_0(i, t) \quad (9)$$

The average mass of the particle can be calculated from the average number of calcium atoms contained in the nucleated particles. The first moment of $n_1(i, t)$ is required for this purpose and can be obtained as

$$\frac{dN_1^{(1)}(t)}{dt} = \sum_{i=1}^{\infty} k_i(t) i n_0(i, t) + qN_1(t) N_0^{(1)}(t) \quad (10)$$

In the above, $N_0^{(1)}(t)$ is the first moment of $n_0(i, t)$ and represents the average number of calcium atoms in non-nucleated micelles. The j th moment of $n_0(i, t)$ is given by

$$N_0^{(j)}(t) = \sum_{i=0}^{\infty} i^j n_0(i, t), \quad j = 1, 2, 3, \dots \quad (11)$$

and can be easily calculated from the Poisson distribution. Similarly, the j th moment of $n_1(i, t)$ is given by

$$N_1^{(j)}(t) = \sum_{i=1}^{\infty} i^j n_1(i, t), \quad j = 1, 2, 3, \dots \quad (12)$$

Toward conserving mass, the calcium atoms gained by nucleated particles due to growth and nucleation must equal the loss of the same from the non-nucleated micelles. Hence,

$$dN_0^{(1)}(t)/dt = -dN_1^{(1)}(t)/dt \quad (13)$$

We shall also estimate the standard deviation in the average size of the particle to compare with the reported values. We need the second moment for this purpose, and it is given by the following equation.

$$\frac{dN_1^{(2)}(t)}{dt} = \sum_{i=1}^{\infty} k_i(t) i^2 n_0(i, t) + q(2N_0^{(1)}(t) N_1^{(1)}(t) + N_0^{(2)}(t) N_1(t)) \quad (14)$$

2.4. Nondimensionalization. Kandori *et al.*³ report number densities normalized with the initial number of micelles, $N_0(0)$. These are given by

$$v_0(t) = N_0(t)/N_0(0) \quad (15)$$

$$v_1(t) = N_1(t)/N_0(0) \quad (16)$$

The higher moments are also nondimensionalized as follows.

$$\mu_1^{(j)}(t) = \frac{N_1^{(j)}(t)}{v_1(t) N_0(0)}, \quad j = 1, 2, 3, \dots \quad (17)$$

$$\mu_0^{(j)}(t) = \frac{N_0^{(j)}(t)}{v_0(t) N_0(0)}, \quad j = 1, 2, 3, \dots \quad (18)$$

The nondimensional moment equations are now written in the following fashion. All the dependent variables are understood to be functions of t . So we do not explicitly mention t in the notation here.

$$\frac{dv_1}{dt} = \sum_{i=1}^{\infty} k_i(t) P_i(t) v_0 \quad (19)$$

$$\frac{dv_0}{dt} = -\sum_{i=1}^{\infty} k_i(t) P_i(t) v_0 - qN_0(0) v_0 v_1 \sum_{i=1}^{\infty} P_i(t) \quad (20)$$

$$\frac{d}{dt}[v_1 \mu_1^{(1)}] = \sum_{i=1}^{\infty} k_i(t) i P_i(t) v_0 + qN_0(0) [v_0 \mu_0^{(1)}] v_1 \quad (21)$$

$$\frac{d}{dt}[v_1 \mu_1^{(2)}] = \sum_{i=1}^{\infty} k_i(t) i^2 P_i(t) v_0 + qN_0(0) v_0 v_1 [\mu_0^{(2)} + 2\mu_0^{(1)} \mu_1^{(1)}] \quad (22)$$

$$\frac{d}{dt}[v_0 \mu_0^{(1)}] = -\frac{d}{dt}[v_1 \mu_1^{(1)}] \quad (23)$$

It may be noted that the moment eq 22 contains $\mu_0^{(2)}$, which is the dimensionless second moment of $n_0(i, t)$. From the assumed Poisson distribution of non-nucleated micelles, the mean of which is $\mu_0^{(1)}$, $\mu_0^{(2)}$ is obtained as follows.

$$\mu_0^{(2)}(t) = \mu_0^{(1)}(t) + [\mu_0^{(1)}(t)]^2 \quad (24)$$

where,

$$\mu_0^{(1)}(t) = \overline{Ca}(t) \quad (25)$$

2.5. Initial Conditions. It remains to specify the initial conditions now. In the beginning none of the micelles are nucleated and hence all moments related to nucleated micelles are zero. The mean number of Ca(OH)₂ molecules per micelle is calculated from the known amount of Ca(OH)₂ taken and the number of micelles existing at the beginning of the experiment. The latter quantity is experimentally obtained by Kandori *et al.*³ the relevant set of initial conditions are as follows.

$$v_1(0) = 0 \quad (26)$$

$$v_0(0) = 1 \quad (27)$$

$$\mu_1^{(1)}(0) = 0 \quad (28)$$

$$\mu_1^{(2)}(0) = 0 \quad (29)$$

$$\mu_0^{(1)}(0) = \begin{cases} 0.0161, & R = 5 \\ 0.0218, & R = 7.5 \\ 0.0372, & R = 10 \\ 0.0671, & R = 15 \\ 0.1308, & R = 20 \end{cases} \quad (30)$$

2.6. Nucleation Rate. Heterogeneous nuclei will not be present in the micelles in view of their small size. The theory of homogeneous nucleation rate can therefore be used. We use the expression for *I*, the rate of nucleation from a condensed phase quoted by Adamson¹⁰ (originally derived by Turnbull and Fisher).

$$I = cA \exp\left(-\frac{\Delta G_{\max}}{k_B T}\right) \quad (31)$$

In the above expression, *I* is the nucleation rate *per unit volume*, *c* is the number concentration of the nucleating molecules in the micellar water pool, and ΔG_{\max} is equal to one-third of the surface free energy for the whole nucleus. The expression for ΔG_{\max} has been given by Gibbs and is quoted by Adamson.¹⁰

$$-\Delta G_{\max} = \frac{16\pi\sigma^3 V_m^2}{3(k_B T)^2 (\ln \lambda)^2} \quad (32)$$

In the above equation λ is the supersaturation with respect to CaCO₃ and is given by

$$\lambda = \left(\frac{[Ca^{2+}][CO_3^{2-}]}{K_s}\right)^{1/2} \quad (33)$$

The other quantities appearing in eq 32 are defined in the Glossary section. The nucleation rate *k_i* in a non-nucleated micelle therefore is obtained by multiplying *I* from eq 31 with the volume of the micelle. However, *c* multiplied by the volume of the micelle is exactly equal to the number of calcium atoms present in the non-nucleated micelle. Hence,

$$k_i = iA \exp\left(-\frac{\Delta G_{\max}}{k_B T}\right) \quad (34)$$

keeping in mind that supersaturation is calculated from eq 33, corresponding to the prevailing concentration of *i* molecules of Ca(OH)₂ in the micelles.

There is however one more complication that has to be resolved before we can calculate nucleation rate. As has been mentioned earlier, there is a distribution in the number of calcium atoms in the non-nucleated micelles, and the actual number of these micelles containing calcium are small. On the other hand, due to the extremely small size of the micelle, the presence of even one atom of calcium makes the atmosphere supersaturated. Thus, even though a finite nucleation rate and hence a finite transition probability to the nucleated state might be predicted for such micelles, it would be unrealistic to expect a nucleus to form with just one calcium atom. Clearly, nucleation can be permitted only in those micelles which possess a minimum number of calcium atoms required to form a nucleus. This number has been reported by several workers for different compounds, and it lies some where between 4 and 6. In this work we have taken it to be 5. On the basis of this consideration, the modified expression for nucleation rate obtained from eqs 32 and 34 is the following.

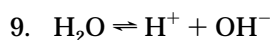
$$k_i = \begin{cases} 0, & i \leq 4 \\ iA \exp\left[-\frac{16\pi\sigma^3 V_m^2}{3(k_B T)^2 (\ln \lambda)^2}\right], & i \geq 5 \end{cases} \quad (35)$$

In eq 35 *A* is a pre-exponential factor, and its precise values are not available. We have used it as an adjustable parameter of the model. Finally to use eq 35, it remains to identify the way supersaturation develops in the micelle. This is done in the following section.

2.7. Supersaturation in the Micelle. When the process begins, the water pool of the micelle contains Ca(OH)₂(aq), Ca²⁺, Ca(OH)⁺, H⁺, and OH⁻. As CO₂ is passed into the solution, it diffuses through the organic phase and is absorbed into the water pool. Consequently, carbonate and bicarbonate ions will be generated in the water pool. The supersaturation in the water pool can be calculated if the concentrations of these ions in the water pool can be predicted as a function of time. To this end, we write mass balance equations for the various species. We consider the following ionic reactions pertinent to CaCO₃ precipitation.

1. $CO_2 + OH^- \rightleftharpoons HCO_3^-$
2. $CO_2 + H_2O \rightleftharpoons HCO_3^- + H^+$
3. $Ca(OH)_2 \rightleftharpoons Ca^{2+} + 2 OH^-$
4. $Ca^{2+} + CO_3^{2-} \rightleftharpoons CaCO_3(aq)$
5. $Ca^{2+} + HCO_3^- \rightleftharpoons CaHCO_3^+$
 $HCO_3^- \rightleftharpoons H^+ + CO_3^{2-}$
6. $H_2CO_3 \rightleftharpoons H^+ + HCO_3^-$

(10) Adamson, A. W. *Physical Chemistry of Surfaces*; John Wiley & Sons: 1990; p 369.



The above nine reactions cover twelve species. Out of these, reactions 1 and 2 involving CO_2 are known to be slow and rate limiting.¹¹ The other seven reactions are ionic in nature and are very fast. They are assumed to be in equilibrium. This then eliminates the need to solve for seven ionic concentrations and leaves one with a reduced system of equations in terms of five conveniently chosen concentration variables. A systematic choice of these five basic variables and the formulation of the reduced set of equations governing the evolution of their concentration with time, together with specification of suitable initial conditions covering mass and charge conservation, have been considered in detail by Gandhi *et al.*¹² and have been followed here.

Kandori *et al.*³ conducted experiments by passing CO_2 for the first 20 s and subsequently nitrogen in order to desorb excess CO_2 . Therefore, the interaction of the continuous organic medium with the micelle by way of transfer of CO_2 has to be accounted for. The equation for the concentration of CO_2 in the water pool is given by

$$\frac{d[\text{CO}_2]}{dt} = -r_1 - r_2 + k_m a_m \left(\frac{S_w}{S_o} [\text{CO}_2]_o - [\text{CO}_2] \right) \quad (36)$$

where we have recognized the rates of the two limiting reactions 1 and 2, involving the absorbed CO_2 . These rates are calculated as follows.

$$r_1 = k_1 \left([\text{CO}_2][\text{OH}^-] - \frac{[\text{HCO}_3^-]}{K_1} \right) \quad (37)$$

$$r_2 = k_2 \left([\text{CO}_2] - \frac{[\text{HCO}_3^-][\text{H}^+]}{K_2} \right) \quad (38)$$

As can be seen, eq 36 is coupled to the concentration of CO_2 in the organic phase. Kandori *et al.*³ have given the rate at which CO_2 has been passed, and those levels were such that all of it was absorbed in the organic phase and none escaped. Therefore, the equation for the concentration of CO_2 in the organic phase is as follows.

$$\frac{d[\text{CO}_2]_o}{dt} = \dot{G} - \frac{V_w}{V_o} k_m a_m \left(\frac{S_w}{S_o} [\text{CO}_2]_o - [\text{CO}_2] \right) \quad (39)$$

In view of the very high interfacial area between the micelles and the organic medium, mass transfer between these two phases can be considered instantaneous, and the concentrations of CO_2 in these two phases will be in equilibrium, related by their respective solubilities. This assumption imparts a further reduction in the number of equations since we can eliminate the concentration of CO_2 in the organic phase in favor of the aqueous phase in the following way. Summing the mass balance eqs 36 and 39 (after multiplying eq 39 by V_o/V_w), we get

$$\frac{d[\text{CO}_2]}{dt} + \frac{V_o}{V_w} \frac{d[\text{CO}_2]_o}{dt} = \frac{V_o}{V_w} \dot{G} - r_1 - r_2 \quad (40)$$

However, due to the equilibrium relationship between the concentrations of CO_2 in the aqueous and organic phases, we have,

$$\frac{d[\text{CO}_2]_o}{dt} = \frac{S_o}{S_w} \frac{d[\text{CO}_2]}{dt} \quad (41)$$

Utilizing eq 41, we eliminate $[\text{CO}_2]_o$ from eq 40 to obtain

$$\frac{d[\text{CO}_2]}{dt} = \frac{-r_1 - r_2 + \frac{V_o}{V_w} \dot{G}}{1 + \frac{S_o V_o}{S_w V_w}} \quad (42)$$

The above equation is valid during the absorption phase. During the desorption phase when nitrogen is being passed, \dot{G} is set to zero and instead we add a term for desorption of CO_2 from the organic phase into the carrier nitrogen gas. Following the same kind of simplifications as described above, we obtain

$$\frac{d[\text{CO}_2]}{dt} = \frac{-r_1 - r_2 - \frac{S_o V_o}{S_w V_w} k_d a [\text{CO}_2]}{1 + \frac{S_o V_o}{S_w V_w}} \quad (43)$$

Therefore, eqs 42 and 43 are to be used during absorption and desorption phases, respectively. The other four equations are ionic mass balances, as given by Gandhi *et al.*¹² (see eq 4.2 of their paper), constituting the previously referred reduced set of five equations in the basic variables. The initial conditions applicable in the present problem are that for an open system, as mentioned by them. Hence,

$$[\text{CO}_2]_{t=0} = 0 \quad (44)$$

$$[\text{CO}_3^{2-}]_{t=0} = 0 \quad (45)$$

The initial values of other three chosen concentration variables differ with R . They are obtained as outlined in Gandhi *et al.*¹² by combining total calcium balance (excluding surfactant CaOT), electroneutrality, and equilibrium constants of reactions 3, 8, and 9. The solution of these ordinary differential equations as an initial value problem furnishes us with all the ionic concentrations in time, which enables us to calculate the changing supersaturation in a non-nucleated micelle.

3. Results and Discussion

Kandori *et al.*³ conducted experiments for all the cases by maintaining a constant molar ratio of surfactant to $\text{Ca}(\text{OH})_2$. In addition, they used a fixed concentration of surfactant dissolved in the organic phase. In order to vary R , they added varied amounts of aqueous solution, which were of different concentration in $\text{Ca}(\text{OH})_2$. However for all R , the micellar water pools contained the same total amount of dissolved $\text{Ca}(\text{OH})_2$, so as to maintain the fixed ratio of surfactant to $\text{Ca}(\text{OH})_2$ in the system. Experimental results have been presented by them for R values of 5, 7.5, 10, 15, and 20. The close proximity of polar surfactant heads with the calcium counterions influences the behavior of water in the micellar water pool and changes its characteristics from the bulk behavior. It is also known that this effect is important for R less than about 10. Thus, it would be inappropriate to use the values measured in bulk water for the thermodynamic

(11) Danckwerts, P. V. *Gas-Liquid Reactions*; McGraw-Hill Book Company: 1970; p 239.

(12) Gandhi, K. S.; Kumar, R.; Ramkrishna, D. *Ind. Eng. Chem. Res.* **1995**, *34*, 3223.

Table 1. Constants of the Model

| constant | value | reference |
|----------|--|-----------|
| K_s | $6.61 \times 10^{-9} \text{ mol}^2 \text{ L}^{-2}$ | 14 |
| k_{ja} | 0.05 s^{-1} | 11 |
| S_w | $0.0389 \text{ mol L}^{-1}$ | 15 |
| S_0 | 0.389 mol L^{-1} | 15 |
| K_1 | $4.4 \times 10^7 \text{ L mol}^{-1}$ | 14 |
| K_2 | $4.4 \times 10^{-7} \text{ mol L}^{-1}$ | 14 |
| k_1 | $6000 \text{ L mol}^{-1} \text{ s}^{-1}$ | 11 |
| k_2 | 0.02 s^{-1} | 11 |
| σ | 97 dyn cm^{-1} | 16 |

Table 2. Process Parameters of Kandori *et al.*³

| item | value |
|--|---|
| $[\text{Ca}(\text{OH})_2] / [\text{CaOT}]$ | 1.67×10^{-3} |
| $[\text{CaOT}]$ | $0.1 \text{ mol/kg organic}$ |
| V_w / V_0 | $1.41 \times 10^{-3} R$ |
| \dot{G} | $5.95 \times 10^{-4} \text{ mol L}^{-1} \text{ s}^{-1}$ |
| total volume of solution | 0.05 L |
| A (fitted value of the nucleation rate) | $2.5 \times 10^{24} \text{ s}^{-1}$ |

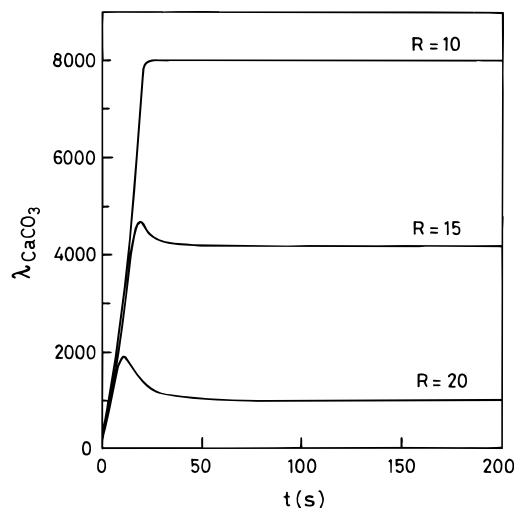
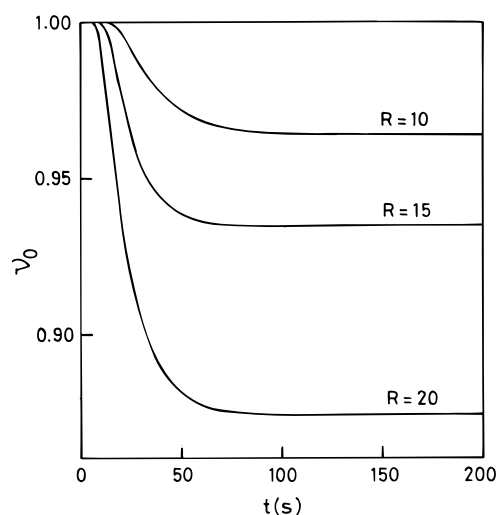
properties of the various components of interest and kinetic and equilibrium constants for the reactions discussed previously. On the other hand, the values for these constants in water pools of small sizes encountered for R less than 10 are not known. So, we can reliably compare the predictions of our model with the experimental results only for R values of 10, 15, and 20.

The nondimensional moment eqs 19–23 for the micelle population, mass balance eqs 42 and 43 for CO_2 , along with the other four ionic mass balance equations together form a set of nonlinear ordinary differential equations in time. The resulting initial value problem was numerically solved using Gears¹³ method. The values of the kinetic and equilibrium constants used in the calculations, together with the sources, are listed in Table 1.

Other process parameters required in the calculations have been provided by Kandori *et al.*³ and are given in Table 2.

The results of the computation yield the various moments as a function of time. This being a batch process, the moments attain a steady value when precipitation comes to an end. As mentioned earlier, Kandori *et al.*³ have measured two quantities at the end of the process. The first of them is the ratio of the initial number of micelles to the final number of particles. The second is mean and variance of the particle size, which is used to obtain the coefficient of variation (COV) in number of molecules composing a particle of CaCO_3 . These correspond to $1/\nu_1$ and $(\mu_1^{(2)} - [\mu_1^{(1)}]^2)^{1/2}/\mu_1^{(1)}$ obtained from the present model. We now present typical results for both the dynamics of the process as well as the terminal values and compare the latter with the experimental values of Kandori *et al.*³

The dynamics of supersaturation in non-nucleated micelles containing the minimum number of calcium atoms required for nucleation to occur is shown in Figure 2 for $R = 10, 15, 20$. It can be seen from there that as the concentration of CO_2 increases due to absorption, supersaturation builds up continuously, reaching a maximum at or prior to 20 s, depending on the value of R . For $R =$

**Figure 2.** Variation of supersaturation of CaCO_3 .**Figure 3.** Number of non-nucleated micelles.

10, supersaturation could have increased further if CO_2 absorption continued. Whereas for $R = 15$ or 20, the maximum is reached within the absorption period itself. Further passage of CO_2 increases HCO_3^- concentration at the cost of CO_3^{2-} and consequently causes a fall in supersaturation up to the end of the absorption period. It is well-known that supersaturation in $\text{Ca}(\text{OH})_2$ solutions of low concentration (*i.e.*, weakly basic solutions) goes through a maximum as the CO_2 concentration increases to its solubility limit. This is because the formation of CO_3^{2-} ion is favored only at high values of pH, *i.e.*, when CO_2 is low. From 20 s onward, as CO_2 is desorbed, formation of CO_3^{2-} is favored again and should increase the supersaturation. However, as desorption is a very slow process, supersaturation remains almost constant during this period.

Figure 3 shows the variation of ν_0 with time for different R values. This is the nondimensional zeroth moment of non-nucleated micelles. At $t = 0$ all the curves show $\nu_0 = 1$, since all the micelles belong to the non-nucleated class. Subsequently, each nucleation event and collision with calcium-containing nucleated micelles decrease the number of this population by one micelle. As a result ν_0 falls, initially rapidly, as both nucleation and growth occurs, and then slowly, when nucleation stops after a while and only growth continues. This plot also gives an idea of the process time, as to when there is no further variation in ν_0 , signalling the termination of growth on consumption of all the $\text{Ca}(\text{OH})_2$. This estimate is around

(13) Gear, C. W. *Numerical initial value problems in ordinary differential equations*; Prentice Hall: Englewood Cliffs, NJ, 1971. The package IVPAG of IMSL subroutines was used in the present work.

(14) Butler, J. N. *Ionic Equilibrium - A Mathematical Approach*; Addison-Wesley Publishing Company: Reading, MA, 1964; p 207.

(15) Hildebrand, J. H.; Scott, R. L. *The solubility of nonelectrolytes*, 3rd ed.; Dover: New York, 1964.

(16) Sangwal, K. J. *Cryst. Growth* **1987**, *97*, 393.

(17) Bommarius, A. S.; Holzwarth, J. F.; Wang, D. I. C.; Hatton, T. *A. J. Phys. Chem.* **1990**, *94*, 7232.

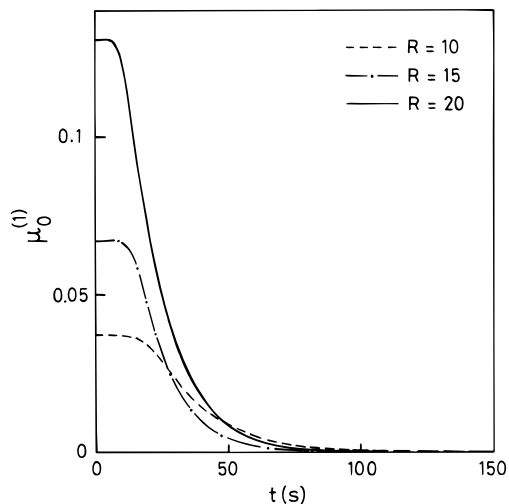


Figure 4. Mean number of $\text{Ca}(\text{OH})_2$ molecules in non-nucleated micelles.

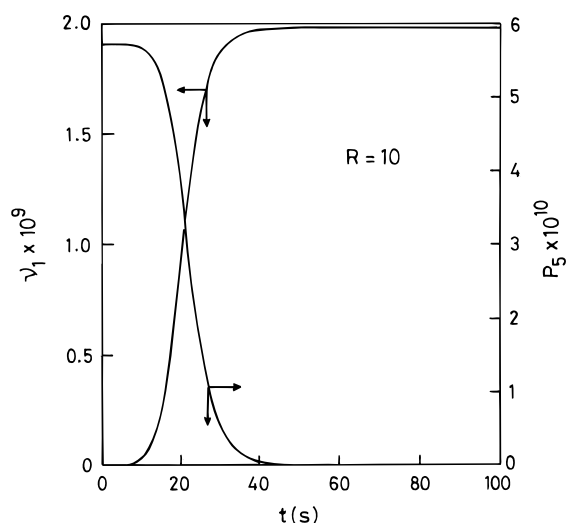


Figure 5. Variation of nondimensional number of nucleated micelles and fraction of non-nucleated micelles containing the minimum number of Ca atoms required to nucleate, $R = 10$.

100 to 80 s as R is increased from 10 to 20. The predicted time is reasonable in view of the reported 20 s of CO_2 absorption period, the total process time having not been reported by Kandori *et al.*³

The dynamics of the average number of calcium atoms in non-nucleated micelles, \bar{C}_a , for $R = 10, 15$, and 20 is shown in Figure 4. For $R = 20$, as the number of micelles is less compared to $R = 10$, the mean number of molecules is initially more in the former, since the total amount of $\text{Ca}(\text{OH})_2$ in the system is same. As expected, \bar{C}_a decreases with time due to precipitation. The decrease begins almost from the very beginning since nucleation in the *entire* system occurs fairly quickly. Like the zeroth moment, the first moment also decreases to a steady value, which should be zero when precipitation is complete.

The fraction of micelles that possess the minimum number of atoms required for nucleation is shown as a function of time in Figures 5–7 for $R = 10, 15$, and 20, respectively. As expected, the fraction decreases with time since \bar{C}_a decreases. In the same figures, the nondimensional number of particles ν_1 has been plotted as a function of time for each R . In all three plots, one observes a similar trend, namely, the two curves are complementary to each other. Initially, as supersaturation takes some time to build up there is no nucleation and no consumption of the micelles also. Subsequently, the nucleation rate begins

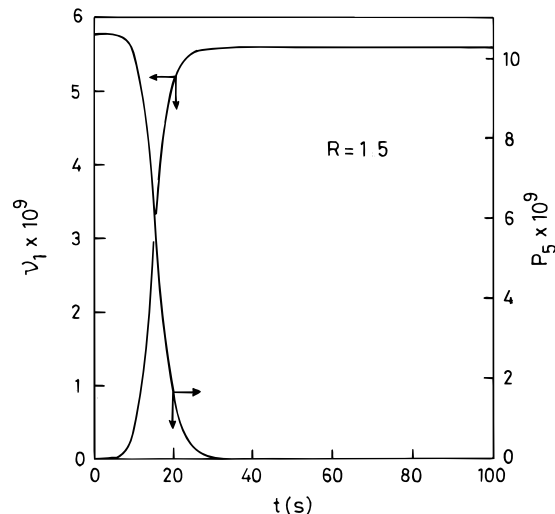


Figure 6. Variation of nondimensional number of nucleated micelles and fraction of non-nucleated micelles containing the minimum number of Ca atoms required to nucleate, $R = 15$.

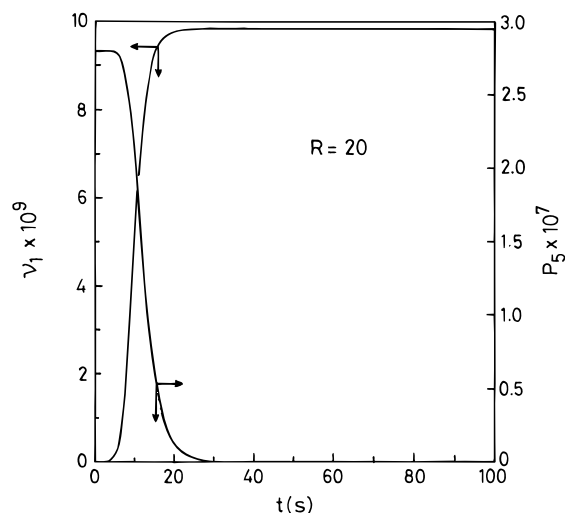


Figure 7. Variation of nondimensional number of nucleated micelles and fraction of non-nucleated micelles containing the minimum number of Ca atoms required to nucleate, $R = 20$.

Table 3. Comparison of Experimental and Predicted Trends of $1/\nu_1$ with R

| R | $1/\nu_1$ (in 10^9) | |
|-----|------------------------|-------|
| | exptl | model |
| 10 | 3.86 | 5.05 |
| 15 | 2.93 | 1.79 |
| 20 | 1.46 | 1.02 |

to pick up causing the fraction of micelles that can nucleate to go down with time. The consequent consumption of calcium due to nucleation and growth further reduces this fraction which in turn slows down the nucleation rate, reflected by an inflexion in the curve giving number of particles. Only for $R = 10$ is there significant nucleation in the desorption period also, because of the high supersaturation (Figure 2).

The experimental observations on the ratio of initial number of micelles to the final number of particles and corresponding predictions from the model, which is given by $1/\nu_1$, are presented in Table 3.

The model suggests that the particle size is determined by the comparative rates of nucleation and fusion, the two processes having opposite effects on particle size. While fusion leads to increased growth and hence size, nucleation enhances the number of particles and hence

decreases the size. Thus very high nucleation rates result in $1/\nu_1$ being close to unity. It can be seen from Table 3 that the predictions agree well with experimental results both in terms of the order of magnitude being 10^8 as well as the decreasing trend with R . This implies that fusion of about 10^8 micelles produces one particle, indicating that collision and fusion is much more prevalent than nucleation in consuming calcium. The important factor working against the high nucleation rate is the nature of distribution of calcium atoms in the micelles. As the initial amount of $\text{Ca}(\text{OH})_2$ in the system is very small, very few micelles containing the required critical number of calcium atoms for nucleation are present (Figures 5–7). As precipitation continues, the fraction of such micelles further goes down. Thus nucleation rate is expected to be small and to decrease further with time. In contrast, micelles which contain one or more calcium atoms, and hence contribute to growth by fusion, are present in much greater abundance. Thus collisions resulting in growth outstrips nucleation rate. Combining together these two effects then, the existence of such a large ratio can be understood.

Consideration of the results of Table 3 shows that the model also captures the decreasing trend in $1/\nu_1$ as one goes from $R = 10$ to $R = 20$. At $R = 10$ the micelles are of smaller diameter compared to those at $R = 20$, but are in more number because of the lower surfactant aggregation number in the former. As far as nucleation is concerned, the same critical number of atoms must be present in a micelle for all the cases. Therefore, the supersaturation in the micelle computed at this critical number of calcium atoms is in decreasing order when R is increased from 10 to 20 because of increasing micelle volume (Figure 2). This would suggest that there should be many more nuclei for $R = 10$ than for $R = 20$. In contrast to this, there is an opposite trend arising out of the distribution of calcium atoms in the micelles. The mean number of calcium atoms increases as R increases from 10 to 20 since a smaller number of micelles exist with increasing R (Figure 4). The Poisson distribution therefore suggests that the micelles at $R = 20$ being larger would have a higher fraction of them containing the required minimum number of calcium atoms for nucleation to occur. This can be seen from Figures 5 to 7. Hence, although the nucleation rate corresponding to the existing supersaturation decreases from $R = 10$ to 20, the probability of nucleation in any given single micelle increases from $R = 10$ to 20. As a result of these two contrasting behaviors, the nucleation rate then becomes almost of the same order, irrespective of R . The fusion rate, however, is proportional to the number of micelles. Now, as there are more micelles present at smaller R , fusion and growth can be expected to be faster for them. The computed ratio, therefore, is greater for smaller R . The model is able to capture this trend with variation in R , though the quantitative agreement is not excellent.

Our task is now to explain the variation observed in the particle size. The model suggests that a distribution in particle size can be generated due to two reasons. Firstly, since growth occurs as a result of random collisions between nucleated and non-nucleated micelles, a distribution in the particle size is generated. Secondly, the distribution operating in the number of $\text{Ca}(\text{OH})_2$ molecules present in the micelles causes each collision to add on a different number of calcium atoms to the existing particles, producing further variation. This later effect is more apparent after nucleation stops, when each collision adds on average more than one calcium atom. The experimental observations would also be influenced, apart from the causes suggested by the model, by the distribution in the micellar size. This aspect, however, has been ignored

Table 4. Comparison of Experimental and Predicted Trends of COV with R

| R | COV | |
|-----|-------|-------|
| | exptl | model |
| 5 | 0.616 | |
| 7.5 | 0.676 | |
| 10 | 0.776 | 0.238 |
| 15 | 0.658 | 0.252 |
| 20 | 0.691 | 0.178 |

in the present model. Experimental values of the mean and standard deviation of the diameter of CaCO_3 particle have been reported, and the distribution has been found to be normal. The present model has been concerned with the number of calcium atoms i present in a particle. Proceeding with the normal distribution then, expressions for the mean and standard deviation of this quantity concerning the number of calcium atoms in a CaCO_3 particle were derived. The coefficient of variation, which is the ratio of standard deviation to mean was then calculated for the experiments. This was then compared with the model predicted COV, according to the following equation.

$$\text{COV} = (\mu_1^{(2)} - [\mu_1^{(1)}]^2)^{1/2} / \mu_1^{(1)} \quad (46)$$

The comparison for different R is shown in Table 4.

Table 4 shows that for R above 7.5, the predicted range of 0.18–0.25 is below the experimentally observed range 0.66–0.78. The complete range of experimental values in Table 4 confirms the absence of any systematic trend in COV with R . However, it is interesting to note that the spread in the distributions for all R values, as given by COV, is nearly constant, and the model also predicts similarly. The implication being on the processes responsible for producing variation, namely nucleation and collision rates, which are getting scaled equally with the experimental parameter R in maintaining the spread in the distribution to nearly constant values.

4. Conclusion

Precipitation of particles in reverse micelles is controlled by the relative rates of various participating processes. In general, particle growth can be treated as instantaneous and a micelle therefore can contain at best a single particle. Thus, in the experiments of Kandori *et al.*,³ where CaCO_3 was precipitated by carbonation of reverse micelles of aqueous $\text{Ca}(\text{OH})_2$ solution, nonempty micelles were either supersaturated or contained a CaCO_3 particle. The final size of the particles formed is then determined by the relative magnitudes of the rate of nucleation and growth occurring by fusion between nucleated and supersaturated micelles. This process could be modeled by a deterministic population balance framework after specifying the minimum number of molecules required to form a nucleus and assuming that interaction between micelles occurs due to Brownian collision and fusion. Experimental measurements by Kandori *et al.*³ on the number of micelles required to form a particle could be predicted successfully, lending some credence to the assumptions made in the model. There exists other complex processes for preparation of fine particles in micellar systems such as that investigated by Roman *et al.*² In their process, precipitation of CaCO_3 and solubilization of micron-sized $\text{Ca}(\text{OH})_2$ particles into reverse micelles occur simultaneously. It would be fruitful to model such processes within the framework developed here. Such models of precipitation processes are important toward the control of particle size in industrial reactors for commercial applications.

Glossary

| | |
|-----------------|---|
| A | pre-exponential factor, s^{-1} |
| \overline{Ca} | mean number of $Ca(OH)_2$ molecules per micelle |
| $[CO_2]$ | concentration of CO_2 in the micellar water pool, $mol\ L^{-1}$ |
| $[CO_2]_o$ | concentration of CO_2 in the organic medium, $mol\ L^{-1}$ |
| \dot{G} | external flow rate of CO_2 , $mol\ L^{-1}\ s^{-1}$ |
| K_s | solubility product of $CaCO_3$, $mol^2\ L^{-2}$ |
| k_B | Boltzman's constant, $1.3806 \times 10^{-16}\ erg\ K^{-1}$ |
| K_1 | equilibrium constant of reaction 1, $L\ mol^{-1}$ |
| K_2 | equilibrium constant of reaction 2, $mol\ L^{-1}$ |
| k_i | homogeneous nucleation rate in a micelle containing i molecules of $Ca(OH)_2$, s^{-1} |
| $k_j a$ | volumetric mass transfer coefficient for CO_2 desorption from water to organic, s^{-1} |
| $k_m a_m$ | volumetric mass transfer coefficient for CO_2 absorption from organic to water, s^{-1} |
| k_1 | forward rate constant of reaction 1, $L\ mol^{-1}\ s^{-1}$ |
| k_2 | forward rate constant of reaction 2, s^{-1} |
| N_0 | total number of non-nucleated micelles per unit volume of dispersion, cm^{-3} |
| $N_0^{(i)}$ | i -th moment of non-nucleated micelle population per unit volume of dispersion, cm^{-3} |
| N_1 | total number of nucleated micelles per unit volume of dispersion, cm^{-3} |
| $N_1^{(i)}$ | i -th moment of nucleated micelle population per unit volume of dispersion, cm^{-3} |
| $n_0(i, t)$ | number of non-nucleated micelles per unit volume of dispersion containing i molecules of $Ca(OH)_2$, cm^{-3} |
| $n_1(i, t)$ | number of nucleated micelles per unit volume of dispersion containing i molecules of $CaCO_3$, cm^{-3} |
| P_i | probability of a micelle containing i molecules of $Ca(OH)_2$ |
| q | Brownian collision frequency of micelles, $cm^{-3}\ s^{-1}$ |
| R | molar ratio of water to surfactant |
| r_1 | rate of first reaction, $mol\ L^{-1}\ s^{-1}$ |
| r_2 | rate of second reaction, $mol\ L^{-1}\ s^{-1}$ |
| S_o | solubility of CO_2 in organic phase, $mol\ L^{-1}$ |
| S_w | solubility of CO_2 in water, $mol\ L^{-1}$ |
| T | temperature of experiment, 298 K |
| t | time, s |
| V_m | volume of a $CaCO_3$ (calcite) molecule, $6.1265 \times 10^{-23}\ cm^3$ |

| | |
|-------|--|
| V_o | total volume of organic phase, cm^3 |
| V_w | total volume of micellar water, cm^3 |

Greek Symbols

| | |
|--------------------|---|
| ΔG_{max} | maximum free energy change during nucleation, |
| λ | supersaturation of any sparingly soluble salt |
| λ_{CaCO_3} | supersaturation of $CaCO_3$ |
| ν_0 | nondimensional number of non-nucleated micelles per unit volume of dispersion |
| ν_1 | nondimensional number of nucleated micelles per unit volume of dispersion |
| η | viscosity of oil medium, $0.009\ g\ cm^{-1}\ s^{-1}$ |
| $\mu_0^{(i)}$ | i -th nondimensional moment of non-nucleated micelle population per unit volume of dispersion |
| $\mu_1^{(i)}$ | i -th nondimensional moment of nucleated micelle population per unit volume of dispersion |
| σ | interfacial tension between nucleus and liquid, $97\ dyn\ cm^{-1}$ |
| τ | time scale of any process, s |

Subscripts

| | |
|------|---------------------------------------|
| 0 | non-nucleated micelle |
| 1 | nucleated micelle |
| n | nucleation in a single micelle |
| nn | nucleation in any micelle |
| c | collision |
| cs | collision with supersaturated micelle |
| cb | collision with blank micelle |
| d | depletion |

Superscripts

| | |
|-----|------------------------------------|
| i | i -th moment of the distribution |
| j | j -th moment of the distribution |

Acknowledgment. The authors gratefully acknowledge the support of the Jawaharlal Nehru Centre for Advanced Scientific Research, Bangalore, India, for making collaboration between D.R. and others possible. D.R. also thanks the International Programs Division of the National Science Foundation for a travel grant in the summer of 1994 during which period this work was initiated.

LA960599+